

# Chemical freeze-out in relativistic heavy-ion collisions

Jun Xu<sup>1,\*</sup> and Che Ming Ko<sup>2,†</sup>

<sup>1</sup>*Shanghai Institute of Applied Physics, Chinese Academy of Sciences, Shanghai 201800, China*

<sup>2</sup>*Cyclotron Institute and Department of Physics and Astronomy,  
Texas A&M University, College Station, Texas 77843, USA*

(Dated: April 18, 2017)

One surprising result in relativistic heavy-ion collisions is that the abundance of various particles measured in experiments is consistent with the picture that they reach chemical equilibrium at a temperature much higher than the temperature they freeze out kinetically. Using a multiphase transport model to study particle production in these collisions, we find that the above result is due to the constancy of the entropy per particle during the evolution of the hadronic matter from the chemical to the kinetic freeze-out. We further use a hadron resonance gas model to illustrate the result from the transport model study.

PACS numbers: 25.75.-q, 24.10.Lx, 24.10.Pa

The statistical model, which assumes that the abundance of particles produced in relativistic heavy-ion collisions or their chemical freeze-out is determined before the hadronic matter freezes out kinetically, has been very successful in describing the yields of particles measured in experiments. For heavy-ion collisions at the top energy of the Relativistic Heavy Ion Collision (RHIC) and the Large Hadron Collider (LHC) [1–3], the chemical freeze-out temperature extracted from the experimental data using the statistical model is around 160 ~ 170 MeV and is similar to the critical temperature of the hadron-quark phase transition from lattice QCD calculation [1–4]. Although it is not known if the chemical freeze-out temperature in the collision energy regime of the RHIC Beam-Energy Scan (BES) program, which is around 140 ~ 160 MeV, coincides with the hadron-quark phase boundary, relativistic heavy-ion collisions provide the only possibility to map out experimentally the phase diagram of the strong-interacting matter in the temperature ( $T$ ) - chemical potential ( $\mu$ ) plane [5]. Since the chemical freeze-out temperature is much higher than that for the kinetic freeze-out, which is around 100 ~ 120 MeV from the blast-wave fit to experimental transverse momentum/mass spectra [6, 7] and slightly decreases with increasing collision energy, to maintain the same relative abundance among various particles requires non-unity values for their fugacities as the hadronic matter expands and cools from the chemical freeze-out temperature  $T_{ch}$  to the kinetic freeze-out temperature  $T_{kin}$ .

To study the origin of early chemical freeze-out, we use a multiphase transport model (AMPT) [8], which has been widely used as a theoretical tool or an event generator for relativistic heavy-ion collisions. In this model, the initial-state information is generated by the Heavy-Ion Jet INteraction Generator (HIJING) model [9], which is an extension of the PYTHIA model [10] for proton-

proton collisions to nucleus-nucleus collisions. In the string melting version of AMPT, which is employed in the present study, all the hadrons produced from HIJING are converted into their valence quarks, and the dynamics of these quarks is described by Zhang’s Parton Cascade (ZPC) model [11]. The parton scattering cross section is set to be 1.5 mb, which has been shown to reproduce reasonably well the experimentally measured collective flow in relativistic heavy-ion collisions [12]. The freeze-out of partons is determined by their last scatterings. Hadrons are then formed from a spatial coalescence mechanism with their species determined by the flavors and invariant mass of their constituent quarks. To reproduce reasonably the empirical energy density and/or temperature near hadronization, we remove the additional hadron formation time of 0.7 fm/c, which was previously introduced to reproduce the hadron multiplicities at midrapidities [8], except the usual one given by  $E/m_T^2$  in terms of the energy  $E$  and transverse mass  $m_T$  of the hadron. The evolution of the hadronic phase is described by a relativistic transport (ART) model [13] that includes various hadron species as well as elastic, inelastic, and decay channels among these hadrons. The empirical energy dependence of the scattering cross sections, the Breit-Wigner mass distribution of resonances, and the mass dependence of the decay width are properly taken into account by satisfying the detailed balance condition, as described in Refs. [8, 13]. The frequent scatterings among hadrons are helpful to maintain the thermal equilibrium in the hadronic phase. In the present work we study central Au+Au collisions at center-of-mass energy  $\sqrt{s_{NN}} = 200$  and 7.7 GeV, corresponding to the top RHIC energy and a typical lower collision energy at the RHIC-BES program where the partonic phase is less dominant. A total number of 100 and 1000 events are generated at  $\sqrt{s_{NN}} = 200$  GeV and 7.7 GeV, respectively.

To give a general picture for particle production in the hadronic phase, we show in Fig. 1 the time evolution of the total number of particles and their formation rate in central Au+Au collisions from the AMPT model. It

\*Electronic address: xujun@sinap.ac.cn

†Electronic address: ko@comp.tamu.edu

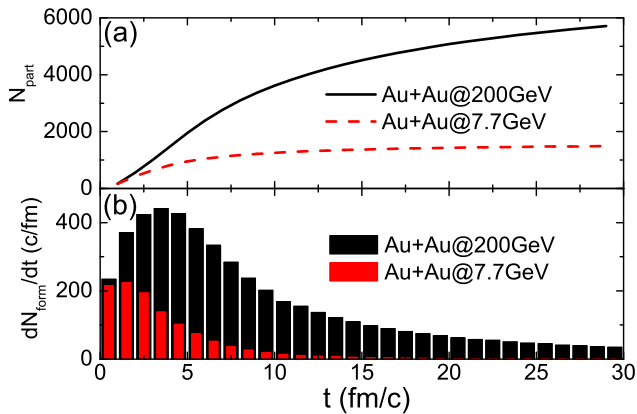


FIG. 1: (Color online). Time evolution of the total number of particles (a) and their formation rate (b) in the hadronic phase of central Au+Au collisions at  $\sqrt{s_{NN}} = 200$  and 7.7 GeV.

is seen that the total number of hadrons increases with time due to the continuous production of hadrons from quark coalescence as well as inelastic and decay channels in the hadronic phase. The different production times of hadrons from quark coalescence are a result of different quark freeze-out times from their last scatterings. Although the final hadron number is much larger at 200 GeV than at 7.7 GeV, hadrons are mostly formed at earlier times at lower collision energies due to the shorter lifetime of the partonic phase.

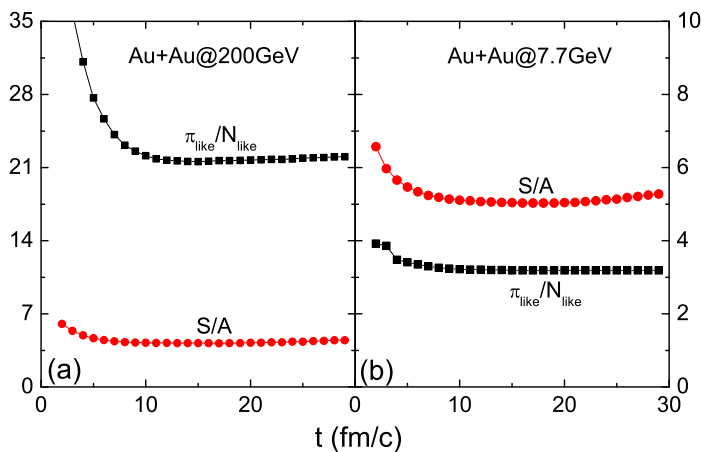


FIG. 2: (Color online). Time evolution of the entropy per particle ( $S/A$ ) and the effective pion/nucleon ratio ( $\pi_{\text{like}}/N_{\text{like}}$ ) in the hadronic phase of central Au+Au collisions at  $\sqrt{s_{NN}} = 200$  (a) and 7.7 GeV (b).

The continuous production of hadrons makes it not possible to define unambiguously the chemical freeze-out time. Instead, we consider the phase-space distribution in the hadronic matter at different times. The resulting time evolution of the effective pion/nucleon ratio is shown

by filled squares in Fig. 2 for collisions at both 200 GeV (left panel) and 7.7 GeV (right panel). In calculating the effective pion/nucleon ratio, we include those from the strong decays of resonances. Specifically, the pion-like particles are pions,  $\Delta$  and  $N^*$  resonances,  $\rho$  mesons,  $\omega$  mesons,  $\eta$  mesons,  $K^*$  mesons, and their antiparticles, while the nucleon-like particles are nucleons and their resonances  $\Delta$  and  $N^*$ .

Since entropy is a thermodynamical quantity that contains information on both the number of degrees of freedom in a system and its degree of thermal equilibration, it is of interest to study this quantity in the hadronic phase of AMPT. Like the viscous effect in hydrodynamic description of heavy-ion collisions [14–17], entropy is produced in AMPT from scattering and production of particles. However, more entropy is expected to be produced in hadronic matter than in partonic matter because of its significantly larger specific viscosity [18]. Based on the thermal model, it has been shown that the entropy per particle in intermediate-energy heavy-ion collisions is related to the deuteron/proton ratio [19, 20]. Therefore, the entropy per particle and relative abundance of particle species in heavy-ion collisions are believed to be related, with the latter often used to extract the information about the former [21, 22]. However, the relation between the entropy per particle and the relative abundance of particles has so far been studied under the assumption that the system is in chemical equilibrium.

In the AMPT, the entropy can be calculated using the phase-space distributions  $f_i(\mathbf{x}, \mathbf{p})$  of particle species  $i$  as in Refs. [23, 24], i.e.,

$$S = - \sum_i g_i \int \frac{d^3\mathbf{x}d^3\mathbf{p}}{(2\pi)^3} [f_i \ln f_i \pm (1 \mp f_i) \ln(1 \mp f_i)], \quad (1)$$

with  $g_i$  being the spin degeneracy of a hadron. For  $f_i$  in the above equation, it is evaluated from counting the number of particles in a local six-dimensional phase-space cell. The size of the phase-space cell is carefully chosen to be small but include sufficient number of particles after averaging over all events [24]. We use spherical coordinates for both position and momentum and divide the phase space into cells. Because of the symmetry in the azimuthal angle for central collisions, the dimension in the phase-space coordinate is reduced. We further introduce a momentum cut of  $|p| < 4$  GeV/c in obtaining the results in Fig. 2 since low-momentum particles dominate at midrapidity. It is seen from Fig. 2 that the entropy per particle and the effective pion/nucleon ratio decrease at the early stage of the hadronic phase, and both become approximately constants at later stage. This behavior is similar to that observed in Ref. [23], where both the pion/nucleon ratio and the entropy per particle remain constant after the most compressed stage in intermediate-energy heavy-ion collisions. Although this result seems to be consistent with the argument that the entropy per particle is related to the relative abundance of particle species at and after chemical freeze-out [19–22], we will show later that the constant entropy per par-

ticle and the constant effective pion/nucleon ratio cannot be achieved simultaneously unless the system becomes out of chemical equilibrium in later stage. However, we can still define the chemical freeze-out time, which is about 8 fm/c at  $\sqrt{s_{NN}} = 200$  GeV and about 6 fm/c at 7.7 GeV, indicated in Fig. 3 by filled squares and circles, respectively, after which the effective pion/nucleon ratio remains essentially unchanged. It is also seen that it takes a longer time to reach chemical freeze-out at 200 GeV than at 7.7 GeV, and this is due to the earlier production of hadrons at lower collision energies as shown in Fig. 1.

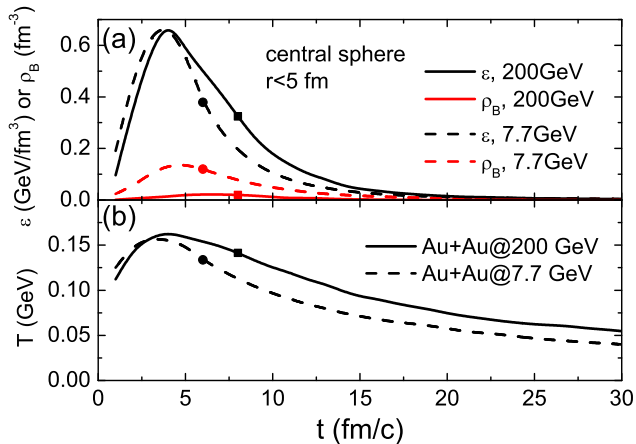


FIG. 3: (Color online). Time evolution of the energy density  $\epsilon$  and the net baryon density  $\rho_B$  (a) in the central sphere of radius  $r = 5$  fm in the hadronic phase of central Au+Au collisions at  $\sqrt{s_{NN}} = 200$  and 7.7 GeV as well as the extracted temperature (b) from the hadron resonance gas model. Filled squares and circles indicate the time after which the effective pion/nucleon ratio and the entropy per particle remain approximately constant.

Results from AMPT, which does not assume thermal and chemical equilibrium, can be qualitatively understood in terms of the hadron resonance gas model that includes all the hadron species in the ART/AMPT model. For such a system containing non-interacting hadrons, the number density  $\rho$ , the energy density  $\epsilon$ , and the entropy density  $s$  can be respectively expressed as [25, 26]

$$\rho = \sum_i g_i \int \frac{d^3p}{(2\pi)^3} f_i, \quad (2)$$

$$\epsilon = \sum_i g_i \int \frac{d^3p}{(2\pi)^3} f_i \sqrt{m_i^2 + p^2}, \quad (3)$$

$$s = - \sum_i g_i \int \frac{d^3p}{(2\pi)^3} [f_i \ln f_i \pm (1 \mp f_i) \ln(1 \mp f_i)], \quad (4)$$

with  $m_i$  being the mass of hadron species  $i$ . The occupation number of hadrons in momentum is given by

$$f_i = \frac{1}{\lambda_i \exp[(\sqrt{m_i^2 + p^2} - \mu_i)/T] \pm 1}, \quad (5)$$

where  $\mu_i = B_i \mu_B + C_i \mu_c$  is the chemical potential of particle species  $i$ , with  $B_i$  and  $C_i$  being its respective baryon and charge numbers,  $\mu_B$  and  $\mu_c$  being its respective baryon and charge chemical potentials, and  $\lambda_i$  is the fugacity that takes into account the possible violation of chemical equilibrium. In the above equations, the upper signs are for Fermions and the lower signs are for Bosons. The charge chemical potential  $\mu_c$  is determined by the charge conservation condition  $\rho_c/\rho_B = 79/197$  for Au+Au collisions, with the charge density  $\rho_c$  and the net baryon density  $\rho_B$  calculated similarly as Eq. (2). The entropy per particle  $S/A$  from the hadron resonance gas model is  $s/\rho$ . Including the same pion-like and nucleon-like particles as in the AMPT calculations and assuming that they are in separate chemical equilibrium, their fugacities can be written as  $\lambda_i = \lambda_N^{z_N} \lambda_\pi^{z_\pi}$ , where  $z_N$  ( $z_\pi$ ) is the effective nucleon (pion) number. For instance, we have  $z_N = 1$  and  $z_\pi = 1$  for  $\Delta$  resonances, and  $z_N = 0$  and  $z_\pi = 2$  for  $\rho$  mesons.

We first evaluate the energy density  $\epsilon$  and the net baryon density  $\rho_B$  in the central sphere of the hadronic phase in AMPT, and the results are shown in the upper panel of Fig. 3. We then use the hadron resonance gas model to obtain from  $\epsilon$  and  $\rho_B$  the temperature, and its time evolution is shown in the lower panel of Fig. 3. The highest energy density of about 0.65 GeV/fm<sup>3</sup> is seen to correspond to the highest temperature of about 152 MeV, which are similar for collisions at both  $\sqrt{s_{NN}} = 200$  and 7.7 GeV. The chemical freeze-out temperature  $T_{ch}$  is 141 MeV at 200 GeV at about  $t = 8$  fm and 134 MeV at 7.7 GeV at about  $t = 6$  fm, which are slightly lower than those extracted from the experimental data based on the statistical model [1, 2, 6, 27, 28].

Using an initial state that is in chemical equilibrium with its thermodynamical properties given by filled symbols in Fig. 3, we have studied the evolution of the entropy per particle, the effective pion/nucleon ratio, the volume expansion rate, and the fugacities of pion-like and nucleon-like particles as the system cools down in a hadron resonance gas model from three different scenarios. In the first scenario shown by filled triangles in Fig. 4, we find that although it is possible to keep the constant effective pion/nucleon ratio by adjusting the volume expansion rate of the hadronic matter, the entropy per particle decreases as the system cools down. In the second scenario shown by filled circles in Fig. 4, we find that it is possible to keep the entropy per particle a constant with a slower volume expansion rate, but the effective pion/nucleon ratio decreases. To keep both the entropy per particle and the effective pion/nucleon ratio constant as in Fig. 2 from the AMPT model, it is necessary to introduce non-unity values for the fugacity parameters. Here we assume that all pion-like and nucleon-like particles are not in chemical equilibrium while their effective numbers remain the same after initial chemical freeze-out. It is seen from the solid lines in Fig. 4 that in this third scenario the system becomes increasingly out of chemical equilibrium during its expansion and cooling

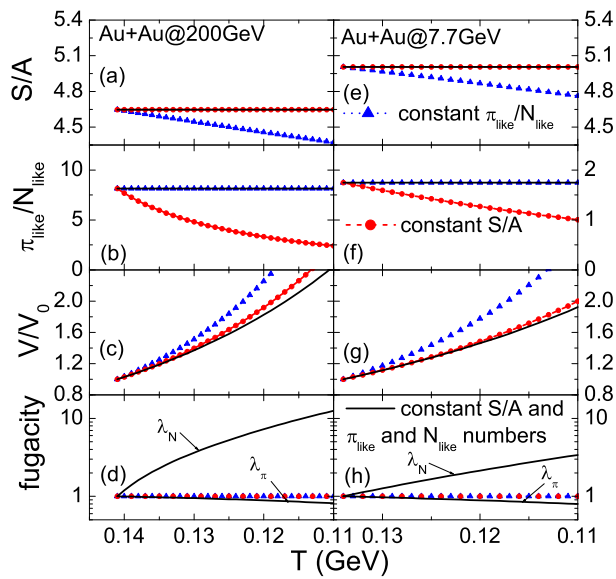


FIG. 4: (Color online). Evolution of the entropy per particle (first row), the effective pion/nucleon ratio (second row), the volume expansion rate (third row), and the fugacities for pion-like and nucleon-like particles (bottom row) as the hadron resonance gas cools with its volume expansion rate and/or the values of particle fugacities varied to keep a constant effective pion/nucleon ratio (filled triangles), a constant entropy per particle (filled circles), or the constancy of both (solid lines). See text for details.

as indicated by increasing nucleon and decreasing pion fugacities away from unity.

To summarize, we have investigated the chemical freeze-out condition in relativistic heavy-ion collisions based on a multiphase transport model. Despite the continuous production of hadrons, the chemical freeze-out time can be determined when the effective pion/nucleon

ratio becomes a constant. The latter is also found to be accompanied by a constant entropy per particle. Starting from the chemical freeze-out state in the AMPT model, we have further studied the expansion and cooling of the system using the hadron resonance gas model, and found that only the scenario of an expanding and cooling hadronic matter with non-unity fugacities can lead to both constant entropy per particle and effective pion/nucleon ratio. Our study shows that after chemical freeze-out in relativistic heavy-ion collisions, the system is no longer in chemical equilibrium, but the statistical model can still be used to extract the temperature and chemical potential at chemical freeze-out since the relative abundances of particle species remain constant during later hadronic evolution. The present study thus helps clarify our understanding of chemical freeze-out in relativistic heavy-ion collisions, and validate the use of the statistical model in mapping out the phase diagram of the strong-interacting matter from relativistic heavy-ion collisions.

We thank Chen Zhong for maintaining the high-quality performance of the computer facility. The work of JX was supported by the Major State Basic Research Development Program (973 Program) of China under Contract Nos. 2015CB856904 and 2014CB845401, the National Natural Science Foundation of China under Grant Nos. 11475243 and 11421505, the "100-talent plan" of Shanghai Institute of Applied Physics under Grant Nos. Y290061011 and Y526011011 from the Chinese Academy of Sciences, the Shanghai Key Laboratory of Particle Physics and Cosmology under Grant No. 15DZ2272100, and the "Shanghai Pujiang Program" under Grant No. 13PJ1410600, while that of CMK was supported by the US Department of Energy under Contract No. de-sc0015266 and the Welch Foundation under Grant No. A-1358.

- 
- [1] J. Adams *et al.* [STAR Collaboration], Nucl. Phys. A **757**, 102 (2005).  
[2] K. Adcox *et al.* [PHENIX Collaboration], Nucl. Phys. A **757**, 184 (2005).  
[3] B. Abelev *et al.* [ALICE Collaboration], Phys. Rev. C **88**, 044910 (2013).  
[4] F. Karsch, Lect. Notes Phys. **583**, 209 (2002).  
[5] Y. Akiba *et al.*, arXiv: 1502.02730 [nucl-th].  
[6] L. Adamczyk *et al.*, arXiv: 1701.07065 [nucl-ep].  
[7] L. Kumer, Nucl. Phys. A **931**, 1114 (2014).  
[8] Z. W. Lin, C. M. Ko, B. A. Li, B. Zhang, and S. Pal, Phys. Rev. C **72**, 064901 (2005).  
[9] X. N. Wang and M. Gyulassy, Phys. Rev. D **44**, 3501 (1991).  
[10] <http://home.thep.lu.se/~torbjorn/Pythia.html>  
[11] B. Zhang, Comput. Phys. Commun. **109**, 193 (1998).  
[12] J. Xu and C. M. Ko, Phys. Rev. C **84**, 014903 (2011).  
[13] B. A. Li and C. M. Ko, Phys. Rev. C **52**, 2037 (1995).  
[14] A. Hosoya and K. Kajantie, Nucl. Phys. B **250**, 666 (1985).  
[15] P. Danielewicz and M. Gyulassy, Phys. Rev. D **31**, 53 (1985).  
[16] H. Heiselberg and X. N. Wang, Phys. Rev. C **53**, 1892 (1996).  
[17] A. Muronga, Phys. Rev. Lett. **88**, 062302 (2002); **89**, 159901(E) (2002); Phys. Rev. C **69**, 034903 (2004).  
[18] N. Demir and S. A. Bass, Phys. Rev. Lett. **102**, 172302 (2009).  
[19] P. J. Siemens and J. I. Kapusta, Phys. Rev. Lett. **43**, 1486 (1979).  
[20] J. Aichelin and E. A. Remler, Phys. Rev. C **35**, 1291 (1987).  
[21] K. G. R. Doss *et al.*, Phys. Rev. C **37**, 163 (1988).  
[22] C. Kuhn *et al.*, Phys. Rev. C **48**, 1232 (1993).  
[23] K. K. Gudima *et al.*, Phys. Rev. C **32**, 1605 (1985).  
[24] G. Bartsch and J. Gunion, Phys. Rev. C **24**, 2514 (1981).  
[25] P. Braun-Munzinger, K. Redlich, and J. Stachel, in: R. Hwa and X. N. Wang (Eds.), Quark Gluon Plasma

- 3, World Scientific, Singapore, 2004, p. 491, arXiv: nucl-th/0304013.
- [26] A. Andronic, P. Braun-Munzinger, and J. Stachel, Nucl. Phys. A **772**, 167 (2006).
- [27] J. Cleymans, H. Oeschler, K. Redlich, and S. Wheaton, Phys. Rev. C **73**, 034905 (2006).
- [28] A. Andronic, P. Braun-Munzinger, and J. Stachel, Nucl. Phys. A **834**, 237c (2010).